Volume 10, Issue 1, June 2023 ISSN 2542-2545

The HIMALAYAN PHYSICS

A peer-reviewed Journal of Physics

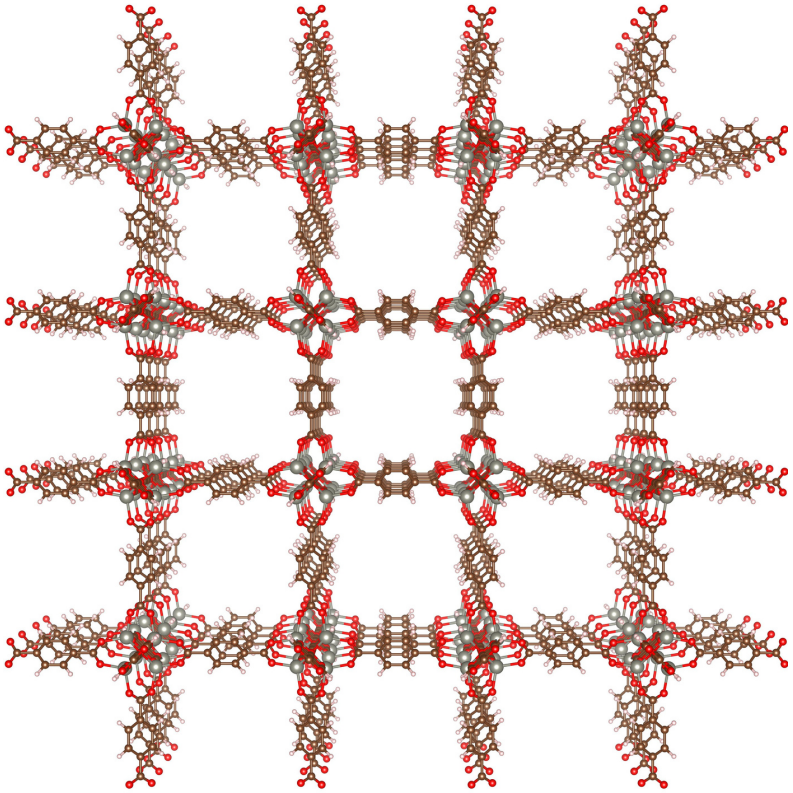

Department of Physics, Prithvi Narayan Campus, Pokhara
Nepal Physical Society, Gandaki Chapter, Pokhara

Publisher

Department of Physics, Prithvinarayan Campus, Pokhara
Nepal Physical Society, Gandaki Chapter, Pokhara

The Himalayan Physics

Volume 10, Issue 1, June 2023

ISSN 2542-2545

The Himalayan Physics (HimPhys) is an open access peer-reviewed journal that publishes quality articles which make innovative contributions in all areas of Physics. HimPhys is published annually by Nepal Physical Society (Gandaki Chapter), and Department of Physics, Prithvi Narayan Campus, Pokhara. The goal of this journal is to bring together researchers and practitioners from academia in Nepal and abroad to focus on advanced techniques and explore new avenues in all areas of physical sciences and establishing new collaborations with physics community in Nepal.

Chief Editor

Aabiskar Bhusal

Cover: Ball-and-stick model of MOF-5. © Roshani Sharma. Printed with permission.

Volume 10, Issue 1, June 2023 ISSN 2542-2545

The HIMALAYAN PHYSICS

A peer-reviewed Journal of Physics

Publisher

Department of Physics, Prithvi Narayan Campus, Pokhara
Nepal Physical Society, Gandaki Chapter, Pokhara

Nepal Physical Society

Gandaki Chapter

Pokhara, Nepal

Himalayan Physics Vol-10(1) (2023)

TABLE OF CONTENTS

****

Him. Phys. **10(1)** 33-39, (2023)

Himalayan Physics

Electronic and magnetic properties of ternary sulfide $Rb_2Mn_3S_4$

Research Article

Gang Bahadur Acharya[1,2] and Madhav Prasad Ghimire[1]*

1 Central Department of Physics, Tribhuvan University, Kirtipur-44613,Kathmandu, Nepal

2 Leibniz-IFW Dresden, Helmholtzstraβe 20, D-01069, Dresden, Germany.

Abstract: Semiconducting materials, especially with a direct band gap, are helpful for modern photovoltaic and optoelectronic device fabrication. Here, based on density functional theory calculations, we predict the electronic and magnetic properties of $Rb_2Mn_3S_4$ by using the full potential local orbital code. Considering different configurations such as nonmagnetic, ferromagnetic, ferrimagnetic, and antiferromagnetic, the magnetic ground state was found to be ferrimagnetic with the lowest total energy. The calculated effective magnetic moment is $10\mu_B$unit cell (two formula units) resulting from the opposite spin interaction between Mn (I) and Mn (II) atoms in $Rb_2Mn_3S_4$. From our calculations, $Rb_2Mn_3S_4$ is found to be a semiconductor with a direct energy band gap of 0.75 eV. With the inclusion of the Coulomb interaction (i.e., GGA+U), the band gap is found to rise to 2.34 eV for U = 4 eV.

Keywords: Density functional theory • Electronic structure • Semiconductor • Magnetism • Density of states • Magnetic moment

I. Introduction

The solid material whose conductivity lies between the insulator and metal is known as a semiconductor. Si and Ge are two well-known elemental semiconductors, whereas GaN GaP, GaSb, GaAs, InSb, GaAsSb, AlGaInP, etc. are some famous examples of compound semiconductors [1]. In compound semiconductors, nonmagnetic (NM), ferromagnetic (FM), antiferromagnetic (AFM) and ferrimagnetic (FIM) semiconductor are extensively studied theoretically as well as experimentally [2]. The magnetic semiconductor research is very attractive, due to its concurrent spontaneous magnetization and semiconducting properties [3–6]. Materials with these qualities are intriguing to microwave devices [7]. The FM semiconducting material La_2NiMnO_6 was reported to be near room temperature based material for spintronics applications. The application of a magnetic field can control the magnetic, electrical, and dielectric properties [8]. Other FM semiconductors which are predicted through the density functional theory (DFT) is $RbLnSe_2$ (Ln = Ce, Pr, Nd,Gd) [9]. Similar to the FM semiconductors, AFM semicondutors are also studied, for instance, S_2IrO_4. It was experimentally observed that Sr_2IrO_4 has anisotropic

* *Corresponding Author: madhav.ghimire@cdp.tu.edu.np*

magnetoresistance [10]. Additionally, a ternary selenide $Na_2Mn_3Se_4$ is a frustrated AFM semiconductor at 27 K. It was reported to have an indirect band gap semiconductor with gap size of 1.59 eV [11]. FIM semiconductors has also been found, such as $CaCu_3Fe_2Sb_2O_{12}$ [12], $CaCu_3Fe_2V_2O_{12}$, $CaCu_3Fe_2Ta_2O_{12}$ [13], and $CaCu_3Mn_4O_{12}$ [14], which has a direct band gap, and can utilized in practical applications for photoelectron materials. The widespread use of magnetic semiconductor can be a result of their excellent efficiency in terms of photocarrier life times. With the numerous number of possible application but less availability of magnetic semiconductor materials, we are motivated to explore magnetic materials with semiconducting character.

In this study, we have used the DFT approach to analyze the electronic and magnetic properties of experimentally synthesized $Rb_2Mn_3S_4$. We predict that the ferrimagnetic semiconductor $Rb_2Mn_3S_4$ can have a net magnetic moment of 10 μ_B per unit cell (two chemical formula unit). With a band gap of 0.75 eV, the material possesses a direct band gap.

II. Methods

We used the full-potential local orbital code (FPLO) [15], version 18.00-52, within the generalized gradient approximation (GGA) and with the inclusion of Coulomb interaction, GGA+U approach. A localized atomic basis and full potential treatment is applied to analyze the electronic band structure and associated characteristics of $Rb_2Mn_3S_4$ using DFT. The exchange-correlation energy functional employed is based on Perdew, Burke, and Ernzerhof's (PBE-96) [16] parameterization. While considering correlation effects, we have used U = 4 eV for our system. A 12 × 12 × 12 k-mesh grid has been used throughout the whole Brillouin zone. The energy convergence criterion was set to 10^{-8} eV for the self-consistent calculations.

III. Results and Discussion

Crystal structures

$Rb_2Mn_3S_4$ (Fig. 1) has been reported to be a body-centered orthorhombic structure with symmetry space group Ibam (space group no. 72). The structure has three dimensions. Eight equivalent S^{2-} atoms form a body-centered cubic geometry connection with Rb^{1+}. There exist two different sites of Mn^{2+}. Mn^{2+} is linked to four equivalent S^{2-} atoms in the initial Mn^{2+} site, creating a mixture of edge and corner-sharing MnS_4 tetrahedra. The experimental lattice parameter of $Rb_2Mn_3S_4$ are $a = 5.84$Å$, b = 11.21$Å$, c = 13.66$Å and angles $\alpha = \beta = \gamma = 90^\circ$, respectively. The atomic Wyckoff positions are [0.268, 0.119, 0.0] for Rb, [0.0, 0.276, 0.25] for Mn(I), [0.0, 0.0, 0.25] for Mn(II), [0.2183, 0.133, 0.344] for S [17].

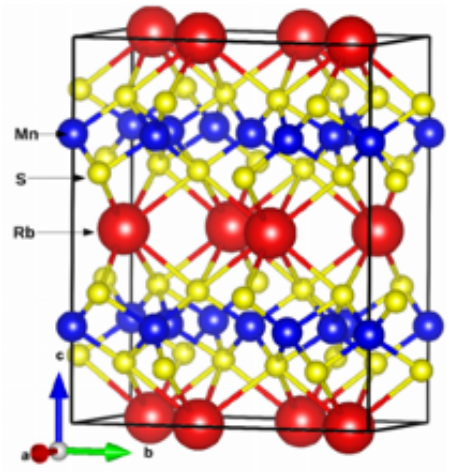

Figure 1. Crystal structure of $Rb_2Mn_3S_4$

Electronic structure

We start with studying the total and partial density of states (DOS) within GGA for the ferrimagnetic ground state, as shown in Fig. 2(a) and Fig. 2(b). A band gap of 0.75 eV is observed between the valence band and the conduction band. The main contributions to the total DOS are seen from the Mn(I)-3d, Mn(II)-3d and S-3p orbitals around E_F. In the conduction region, S-3p and Mn(II)-3d dominate above E_F in spin-up channels, while in spin-down, Mn(I)-3d has significant contributions. On the other hand, below E_F, Mn(I)-3d states significantly contribute to spin-up, while the spin-down channel is contributed by Mn(II)-3d hybridizing with the S-3p states. Generally, the DFT technique underestimates the size of the electronic band gap. To resolve this issue, we apply the Hubbard parameter (U), which plays a significant role in handling the delocalized d-bands resulting in the correct prediction of the experimental band gap. This was done following the literatures [11, 18–20] , which suggests that the appropriate value of U for Mn is between 3 and 4 eV in most cases. We thus report our result using 4 eV. The total and partial DOS within GGA+U is shown in Fig. 2(c) and Fig. 2(d). Interestingly, the Mn-3d states below E_F shift far below, with some minor states around E_F hybridizing significantly with the S-3p states. The band gap so formed is of charge-type between the Mn(I) and S-3p states. Focusing now on the electronic band structure of $Rb_2Mn_3S_4$ in scalar relativistic mode (see fig. 3(a,b)), both the valence band maximum (VBM) and the conduction band minimum (CBM) lies at the high-symmetry point Z in the momentum space dictating that the material $Rb_2Mn_3S_4$ is a direct band semiconductor. This suggests that electrons can transfer straight from the VBM to the CBM. In particular, the band gap makes $Rb_2Mn_3S_4$ an attractive choice for photovoltaic and optoelectronic devices due to the finite gap size within the visible range [13]. The calculated energy gap within GGA and GGA+U are 0.75 and 2.34 eV, respectively.

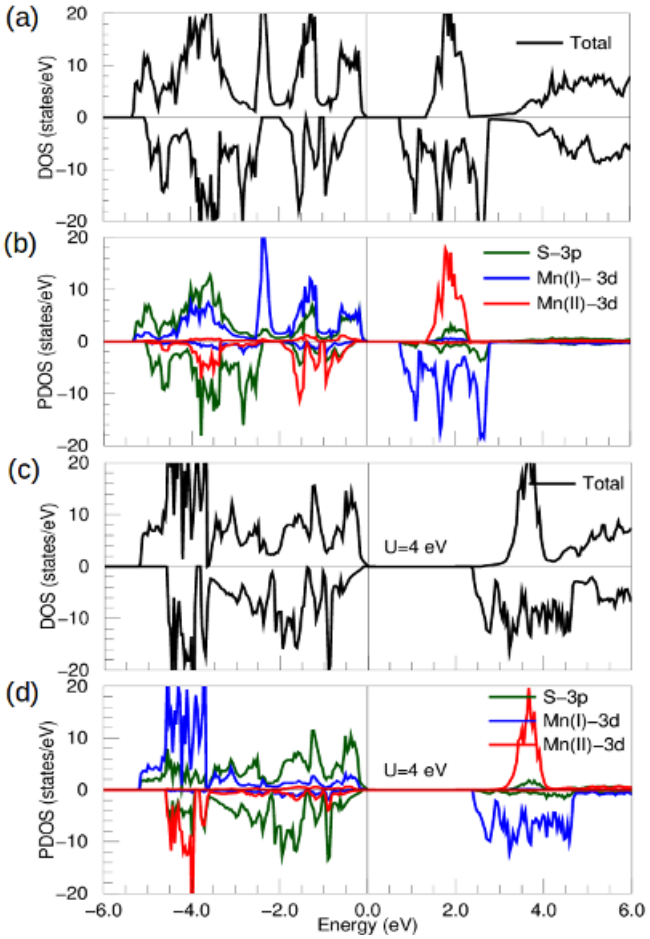

Figure 2. Total and partial DOS of $Rb_2Mn_3S_4$ in scalar relativistic mode within GGA and GGA+U (with U=4 eV for Mn).

We further calculate the band gap considering U (for Mn) ranging from 1 to 6 eV. Interestingly, with increased U, the electronic band gap is shown in Fig. 4. For U = 4 eV, we observed a direct band gap of 2.34 eV.

Magnetic properties

From the total energy calculations, the ferrimagnetic (FIM) configuration is the magnetic ground state with a total energy difference of 2.6 eV between the FM and FIM states. In the FIM configuration, two inequivalent Mn atoms MnI and Mn(II), align antiferromagnetically as Mn(I)↑-Mn(II)↓ interacting with each other via Sn-3p orbitals. The calculated effective magnetic moments is 10 μ_B/unit cell with an individual moment of 4.4 μ_B for Mn(I) and 4.1 μ_B for Mn(II), with polarized moment transfer to Sn (0.07 μ_B) atoms. However, the effective magnetic moment within GGA+U remains the same (10 μ_B/unit cell) as that of GGA; the individual moment rises slightly to 4.8 μ_B and 4.7 μ_B for Mn(I) and Mn(II), mainly due to correlation effects. We further consider the relativistic effect (spin-orbit coupling) to identify the magnetic easy axis along [001], [010], and [100] directions.

The magnetic easy axis was found along [010] while the hard axis is along [100] direction. The calculated magnetic anisotropic energy is ∼0.4 meV per unit cell, suggesting the minimal effect of spin-orbit coupling in $Rb_2Mn_3S_4$.

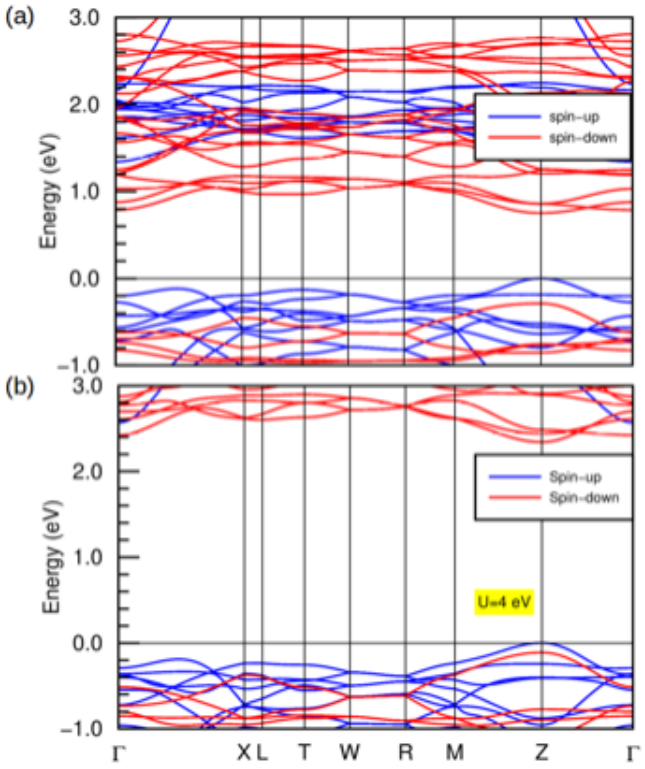

Figure 3. Electronic band structure of $Rb_2Mn_3S_4$ in scalar relativistic mode for GGA and GGA+U (with U=4 eV for Mn). The Fermi level is set to zero.

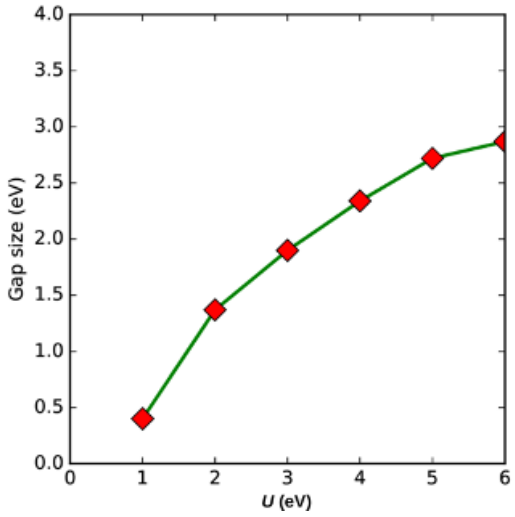

Figure 4. Calculated gap size with the changing value of U in $Rb_2Mn_3S_4$

IV. Conclusions

Using the density functional theory approach, we investigate the electronic structure and magnetic properties of $Rb_2Mn_3S_4$. The material is found to be a direct band gap magnetic semiconductor with a gap size of 0.75 eV within GGA. The ferrimagnetic $Rb_2Mn_3S_4$ has a total magnetic moment of $10\mu_B$/unit cell. Identifying new magnetic direct band gap semiconductors opens the door for additional experimental research for this group of materials that could be used to fabricate valuable devices, including semiconductor lasers, solar cells, and light-emitting diodes.

V. Acknowledgements

G.B.A. and M.P.G. thanks PD Dr. Manuel Richter, IFW-Dresden, for the fruitful discussion and suggestions. M.P.G. was supported by a grant from UNESCO-TWAS and the Swedish International Development Cooperation Agency (SIDA). The views expressed herein do not necessarily represent those of UNESCO-TWAS, SIDA, or its Board of Governors. G.B.A. thanks the Nepal Academy of Science and Technology for the Ph.D. fellowship. M.P.G. and G.B.A. thanks Ulrike Nitzsche for the technical assistance.

References

[1] Kasap SO, Capper P. Springer handbook of electronic and photonic materials. vol. 11. Springer; 2006.

[2] Hall KC, Lau WH, Gündoğdu K, Flatté ME, Boggess TF. Nonmagnetic semiconductor spin transistor. Applied Physics Letters. 2003;83(14):2937-9.

[3] Ohno H. Making nonmagnetic semiconductors ferromagnetic. science. 1998;281(5379):951-6.

[4] Dietl T. A ten-year perspective on dilute magnetic semiconductors and oxides. Nature materials. 2010;9(12):965-74.

[5] Matthias B, Bozorth R, Van Vleck J. Ferromagnetic interaction in EuO. Physical Review Letters. 1961;7(5):160.

[6] Baltzer P, Lehmann H, Robbins M. Insulating ferromagnetic spinels. Physical Review Letters. 1965;15(11):493.

[7] Shlyk L, Strobel S, Farmer B, De Long LE, Niewa R. Coexistence of ferromagnetism and unconventional spin-glass freezing in the site-disordered kagome ferrite SrS n 2 F e 4 O 11. Physical Review B. 2018;97(5):054426.

[8] Rogado NS, Li J, Sleight AW, Subramanian MA. Magnetocapacitance and magnetoresistance near room temperature in a ferromagnetic semiconductor: La2NiMnO6. Advanced Materials. 2005;17(18):2225-7.

[9] Azzouz L, Halit M, Charifi Z, Baaziz H, Rérat M, Denawi H, et al. Magnetic semiconductor properties of RbLnSe2 (Ln= Ce, Pr, Nd, Gd): a density functional study. Journal of Magnetism and Magnetic Materials.

2020;501:166448.

[10] Fina I, Marti X, Yi D, Liu J, Chu J, Rayan-Serrao C, et al. Anisotropic magnetoresistance in an antiferromagnetic semiconductor. Nature communications. 2014;5(1):4671.

[11] Pak C, Garlea VO, Yannello V, Cao H, Bangura AF, Shatruk M. Na2Mn3Se4: Strongly Frustrated Antiferromagnetic Semiconductor with Complex Magnetic Structure. Inorganic Chemistry. 2019;58(9):5799-806.

[12] Xiang H, Wang J, Meng J, Wu Z. Ferrimagnetic and semiconducting CaCu3Fe2Sb2O12 by first principles. Computational materials science. 2009;46(2):307-9.

[13] Li H, Ge Z, Sun A, Zhu Z, Tian Y, Lv S. Ferrimagnetic semiconductor of CaCu3Fe2V2O12 with direct bandgap. Chemical Physics Letters. 2020;759:137910.

[14] Weht R, Pickett WE. Magnetoelectronic properties of a ferrimagnetic semiconductor: The hybrid cupromanganite CaCu 3 Mn 4 O 12. Physical Review B. 2001;65(1):014415.

[15] Koepernik K, Eschrig H. Full-potential nonorthogonal local-orbital minimum-basis band-structure scheme. Physical Review B. 1999;59(3):1743.

[16] Perdew JP, Burke K, Ernzerhof M. Generalized gradient approximation made simple. Physical review letters. 1996;77(18):3865.

[17] Bronger W, Böttcher P. About thiomanganates and cobaltates of heavy alkali metals: Rb2Mn3S4Cs2Mn3S4Rb2Co3S4Cs2Co3S4. Journal of inorganic and general chemistry. 1972;390(1):1-12.

[18] Boukhvalov D, Solovyev I. Defects of the crystal structure and Jahn-Teller distortion in BiMnO 3. Physical Review B. 2010;82(24):245101.

[19] Tolba SA, Gameel KM, Ali BA, Almossalami HA, Allam NK. The DFT+ U: Approaches, accuracy, and applications. Density Functional Calculations-Recent Progresses of Theory and Application. 2018;1:5772.

[20] Tran F, Blaha P, Schwarz K, Novák P. Hybrid exchange-correlation energy functionals for strongly correlated electrons: Applications to transition-metal monoxides. Physical Review B. 2006;74(15):155108.